Available online at www.sciencedirect.com
SCIENCE DIRECT®
Mutation Research 603 (2006) 151–158
Genetic Toxicology and Environmental Mutagenesis
www.elsevier.com/locate/gentox
Community address: www.elsevier.com/locate/mutres

Genotoxicity of acrylamide and glycidamide in human lymphoblastoid TK6 cells

Naoki Koyama [a,b,c], Hiroko Sakamoto [a], Mayumi Sakuraba [a], Tomoko Koizumi [a], Yoshio Takashima [a], Makoto Hayashi [a], Hiroshi Matsufuji [b], Kazuo Yamagata [b], Shuichi Masuda [c], Naohide Kinae [c], Masamitsu Honma [a,*]

[a] *Division of Genetics and Mutagenesis, National Institute of Health Sciences, 1-18-1 Kamiyoga, Setagaya-ku, Tokyo 158-8501, Japan*
[b] *Department of Food Science and Technology, College of Bioresource Sciences, Nihon University, 1866 Kameino, Fujisawa-shi, Kanagawa 252-8510, Japan*
[c] *Laboratory of Food Hygiene, Graduate School of Food and Nutritional Sciences, University of Shizuoka, 52-1 Yada, Suruga-ku, Shizuoka 422-8526, Japan*

Received 14 June 2005; received in revised form 6 October 2005; accepted 22 November 2005
Available online 18 January 2006

Abstract

The recent finding that acrylamide (AA), a potent carcinogen, is formed in foods during cooking raises human health concerns. In the present study, we investigated the genotoxicity of AA and its metabolite glycidamide (GA) in human lymphoblastoid TK6 cells examining three endpoints: DNA damage (comet assay), clastogenesis (micronucleus test) and gene mutation (thymidine kinase (*TK*) assay). In a 4 h treatment without metabolic activation, AA was mildly genotoxic in the micronucleus and *TK* assays at high concentrations (>10 mM), whereas GA was significantly and concentration-dependently genotoxic at all endpoints at ≥0.5 mM. Molecular analysis of the *TK* mutants revealed that AA predominantly induced loss of heterozygosity (LOH) mutation like spontaneous one while GA-induced primarily point mutations. These results indicate that the genotoxic characteristics of AA and GA were distinctly different: AA was clastogenic and GA was mutagenic. The cytotoxicity and genotoxicity of AA were not enhanced by metabolic activation (rat liver S9), implying that the rat liver S9 did not activate AA. We discuss the in vitro and in vivo genotoxicity of AA and GA.

Keywords: Acrylamide; Gycidamide; Genotoxicity; *TK* mutation; Metabolic activation

1. Introduction

Acrylamide (AA) is a synthetic chemical that has been produced since the early 1950s. Because AA polymerizes easily to an adhesive gel, it has been widely used in industry for water flocculation, soil coagulation and grouts. Because it had been believed that humans are rarely exposed to AA under ordinary circumstances, concern was centered only on occupational exposure [1]. In 2000, however, Tareke et al. [2] reported that AA was unexpectedly discovered in cooking foods. It forms during frying and baking principally by a Maillard reaction between asparagine residues and glucose [3,4]. This finding raises concerns about the health risks of AA for the general population [5].

According to toxicological studies, AA is neurotoxic for animals and human [6,7], and the International

* Corresponding author. Tel.: +81 3 3700 1141x434; fax: +81 3 3700 2348.
E-mail address: honma@nihs.go.jp (M. Honma).

1383-5718/$ – see front matter © 2005 Elsevier B.V. All rights reserved.
doi:10.1016/j.mrgentox.2005.11.006

Agency for Research on Cancer classifies it as 2A, a probable human carcinogen [1]. AA is also genotoxic in somatic and germinal cells in in vitro and in vivo [8]. In vivo examination [8] AA is metabolized to the epoxide derivative glycidamide (GA), presumably by cytochrome P4502E1 (CYP2E1) [9]. GA may be more toxic than AA because it reacts quickly with DNA and other biological macromolecules, and it is positive in most genotoxicity tests [8]. AA, on the other hand, is inactive in bacterial and some in vitro mammalian gene mutation assays, but it induces sister chromatid exchanges and chromosome aberrations in vitro and in vivo [8]. AA may have indirect genotoxic mechanisms, such as protein binding, spindle disturbance or hormonal imbalance, which could lead to tumors [10,11]. Thus, the genotoxic mechanism of AA is unclear.

In the present study, we used human lymphoblatoid TK6 cells to investigate the genotoxicity of AA and GA and its mechanisms. TK6 cells are widely used for the thymidine kinase (*TK*) gene mutation assay and can also be used in the in vitro micronucleus (MN) and comet (COM) assays. The *TK* gene mutation assay detects a wide range of genetic damage, including gene mutations, large-scale chromosomal deletions, recombination and aneuploidy [12], while other mammalian gene mutation assays, such as the *HPRT* and transgenic *LacZ* and *LacI* gene assays, detect only point mutations and small deletions [13]. Most of the genetic changes observed in *TK* mutants occur in human tumors and are presumably relevant to carcinogenesis. Molecular analysis of the TK mutants induced by AA or GA can help elucidate their genotoxic mechanisms. In addition, because it uses a human cell line, the *TK* assay is appropriate for human hazard evaluation.

2. Materials and methods

2.1. Cell culture, chemicals and treatment

The TK6 human lymphoblastoid cell line has been described previously [14]. The cells were grown in RPMI1640 medium (Gibco-BRL, Life technology Inc., Grand Island, NY) supplemented with 10% heat-inactivated horse serum (JRH Biosciences, Lenexa, KS), 200 μg/ml sodium pyruvate, 100 U/ml penicillin and 100 μg/ml streptomycin and maintained at 10^5 to 10^6 cells/ml at 37 °C in a 5% CO_2 atmosphere with 100% humidity.

AA (CAS # 79-06-1) and GA (CAS # 5694-00-8) were purchased from Wako Pure Chemical Co. (Tokyo). We dissolved them in phosphate-buffered saline just before use. *N*-di-*N*-butylnitrosamine (DBN) (CAS # 924-16-3) was purchased from Tokyo Kasei Kogyo Co. Ltd. (Tokyo) and dissolved in DMSO for use. Post-mitochondrial supernatant fractions of liver homogenate (S9) were purchased from Kikkoman Co. Ltd. (Noda, Chiba, Japan), which were prepared from the liver of phenobarbital- and 5,6-benzoflavone-treated SD rats. We prepared a 10 ml S9 mix with 4 ml S9 fraction and 2 ml each of 180 mg/ml glucose-6-phosphate, 25 mg/ml NADP and 150 mM KCl.

We treated 20 ml aliquots of cell suspensions (5.0×10^5 cells/ml) at 37 °C for 4 h with serially diluted AA or GA, washed them once, re-suspended them in fresh medium, and cultured them in new flasks for the MN and *TK* assays or diluted and plated them for survival measurement (PE0). We treated the cultures with AA both in the absence and presence of 5% S9 mix.

2.2. Comet assay

After treating the cells for 4 h with AA or GA, we prepared slides for alkaline COM assay as previously reported [15]. Briefly, the cells were suspended in 0.5% agarose-LGT (Nakalai Tesque Inc., Kyoto, Japan), quickly layered on a slide (Matsunami Glass Ind. Ltd., Osaka, Japan) coated with 1% agarose GP-42 (Nakalai Tesque Inc.), and covered with 0.5% agarose-LGT. We immersed the slide in alkaline lysing solution (pH 13) for 1 h, electrophoresed it for 15 min after the unwinding treatment, fixed the cells with 70% ethanol, and stained them with SYBER green (Molecular Probes, Eugene, OR) according to the manufacturer's recommendation. We observed the cells by an Olympus model BX50 fluorescence microscope. At least 50 cells were captured by CCD camera, and the tail length of the comet image was measured. We statistically analyzed the difference between the non-treated and treated plates with the Dunnett's test after one-way ANOVA [16].

2.3. Micronuclei test

Forty-eight hours after treatment, we prepared the MN test samples as previously reported [17]. Briefly, approximately 10^6 cells suspended in hypotonic KCl solution were incubated for 10 min at room temperature, fixed twice with ice-cold glacial acetic acid in methanol (1:3), and resuspended in methanol containing 1% acetic acid. We placed a drop of the suspension on a clean glass slide and allowed it to air-dry. We stained the cells with 40 μg/ml acridine orange solution and immediately observed them by Olympus model BX50 fluorescence microscope. At least, 1000 intact interphase cells for each treatment were examined, and the cells containing MN were scored. The MN frequencies between non-treated and treated cells were statistically analyzed by Fisher's exact test. The concentration–response relationship was evaluated by the Cochran–Armitage trend test [18].

2.4. TK gene mutation assay

The TK6 cell cultures were maintained for 3 days after treatment to permit expression of the *TK* deficient phenotype. To isolate the *TK* deficient mutants, we seeded cells from each

culture into 96-microwell plates at 40,000 cells/well in the presence of 3.0 μg/ml trifluorothymidine (TFT). We also plated them at 1.6 cells/well in the absence of TFT for the determination of plating efficiency (PE3). All plates were incubated at 37 °C in 5% CO_2 in a humidified incubator. The TK assay produces two distinct phenotypic classes of *TK* mutants: normally growing (NG) mutants had the same doubling time (13–17 h) as the wild type cells, and slowly growing (SG) mutants had a doubling time of >21 h. The difference is thought to be due to a putative gene near the *TK* gene. NG mutants result mainly from intragenic mutations, such as point mutations and small deletions, while SG mutants result from gross genetic changes extending beyond the *TK* gene [19]. We scored for the colonies in the PE plates and for the colonies for normal-growing *TK* mutants in the TFT plates at 14th day after plating. We then refed the plates containing TFT with fresh TFT, incubated them for an additional 14 days, and scored them for slow-growing *TK* mutants. Mutation frequencies were calculated according to the Poisson distribution [20]. The data were statistically analyzed by Omori's method, which consists of a modified Dunnett's procedure for identifying clear negative, a Simpson–Margolin procedure for detecting downturn data, and a trend test to evaluate the dose-dependency [21].

2.5. Molecular analysis of TK mutants

Genomic DNA was extracted from *TK* mutant cells and used as a template for the polymerase chain reaction (PCR). We analyzed for loss of heterozygosity (LOH) at the human *TK* gene by PCR products as described previously [22]. A set of primers was used to each amplify the parts of exons 4 and 7 of the *TK* gene that contains frameshift mutations. Another primer set for amplifying parts of the β-globin were also prepared. We used quantitative-multiple PCR to co-amplify the three regions and to identify and quantify the PCR products. We analyzed them with an ABI310 genetic analyzer (PE Biosystems, Chiba, Japan), and classified the mutants into "none LOH", "hemizygous LOH" or "homozygous LOH". To determine the extent of LOH, we analyzed 10 microsatellite loci on chromosome 17q by PCR-based LOH analysis described previously [22]. The results were processed by GenoTyper™ software (PE Biosystems) according to the manufacturer's guidelines.

3. Results

3.1. Cytotoxic and genotoxic responses to AA and GA

Fig. 1a shows the effect of AA on relative survival (RS), mutation frequency (*TK* assay) and number of micronucleated cells per 1000 cells examined. AA was concentration-dependently cytotoxic, permitting about 20% RS at the maximum concentration (14 mM), while its genotoxicity and clastogenicity were weak. We repeated the experiment because of the weak genotoxicity. AA showed negative in the first *TK* assay, but positive in the second statistically. In MN test, both experiments showed statistically positive. GA, in contrast, was significantly genotoxic even at concentrations that were not severely cytotoxic (Fig. 1b). At the maximum concentration (2.4 mM), GA induced *TK* mutation frequencies that were about 20 times and MN fre-

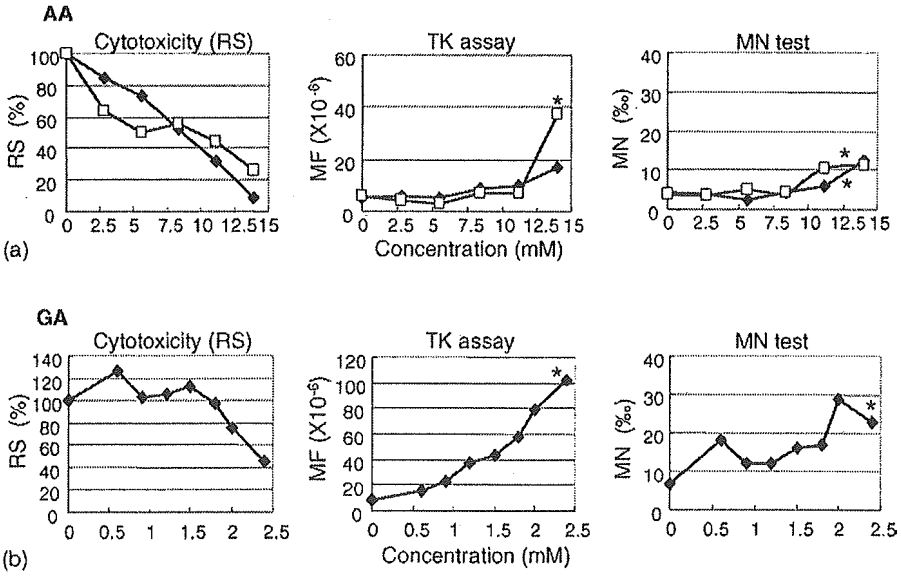

Fig. 1. Cytotoxic (relative survival, RS), genotoxic responses (TK assay and MN test) of TK6 cells treated with AA (a) or GA (b) for 4 h without metabolic activation. The AA experiment was repeated to confirm the result because of the weak genotoxicity. Closed and open symbols are first and second experiment, respectively. Asterisk (*) statistically significant experiments in both pair-wise comparison and trend test ($P < 0.05$).

Table 1
Cytotoxic and mutational responses to AA and GA, and the results of LOH analysis of normally growing (NG) and slowly growing (SG) TK-mutants

Treatment	Cytotoxic and mutational response			LOH analysis at TK gene			
	RS (%)	MF ($\times 10^{-6}$)	% SG	No.	None LOH	Hemi-LOH	Homo-LOH
Vehicle [16]	100	2.19	56	56			
NG mutants				19	14 (74)	3 (16)	2 (11)
SG mutants				37	0 (0)	9 (24)	28 (76)
AA (14 mM, 4 h)	40	18.9	54	48			
NG mutants				22	11 (50)	11 (50)	0 (0)
SG mutants				26	0 (0)	13 (50)	13 (50)
GA (2.2 mM, 4 h)	12	55.5	36	44			
NG mutants				28	26 (93)	2 (7)	0 (0)
SG mutants				16	0 (0)	6 (38)	10 (62)

quencies at about four times the spontaneous level. We detected two distinct phenotypic classes of *TK* mutants in *TK* assay: NG and SG mutants. AA did not affect the proportion of SG mutants, while GA treatment lowered it (Table 1). This implies that GA induced primarily point mutations. In the COM assay, even at the highest concentration, AA did not induce DNA damage, while GA did so strongly starting at 0.6 mM (Fig. 2).

3.2. Molecular analysis of TK mutants

The *TK* mutants were independently isolated from the cells treated with 14 mM AA or 2.2 mM GA for 4 h. Table 1 shows the cytotoxicity (RS) and *TK* mutation frequency (MF) and proportion of SG mutants (% SG) by the treatment. Genomic DNA extracted from the mutants was subjected by the PCR-based LOH analysis to classify the mutants into three types: non-LOH, hemizygous LOH (hemi-LOH) and homozygous LOH (homo-LOH). In general, hemi-LOH is resulted by deletion and homo-LOH is by inter-allelic homologous recombination [13]. We analyzed 48 AA-induced and 44 GA-induced *TK* mutants and compared them to those of spontaneously occurring *TK* mutants described previously [16]. The fraction of hemi-LOH in AA-induced mutants, in which 50% each of NG and SG mutants exhibited hemi-LOH, was higher than in spontaneous mutants, indicating that AA-induced primarily deletions. GA, on the other hand, induced primarily NG mutants, and most (93%) of them were the non-LOH type, which is presumably generated by point and other small intragenic mutations. Among 16 GA-induced SG mutants, the percentages that were hemi-LOH (38%) and homo-LOH (62%) were similar to those observed in spontaneous SG mutants. Fig. 3 shows the mutation spectra of *TK* mutants found among treated and untreated TK6 cells. GA and ethyl methane sulfonate, an alkylating agent, produce similar spectra, as do AA and X-radiation.

Fig. 4 shows the distribution of LOH in AA-induced ($n=37$), GA-induced ($n=17$) and spontaneous ($n=29$) LOH mutants. Because the majority of GA-induced mutants were the non-LOH type, we were able to map only 17 GA-induced LOH mutants. As a particular characteristic of AA-induced LOH mutants, we frequently observed small deletions limited to the *TK* locus. The

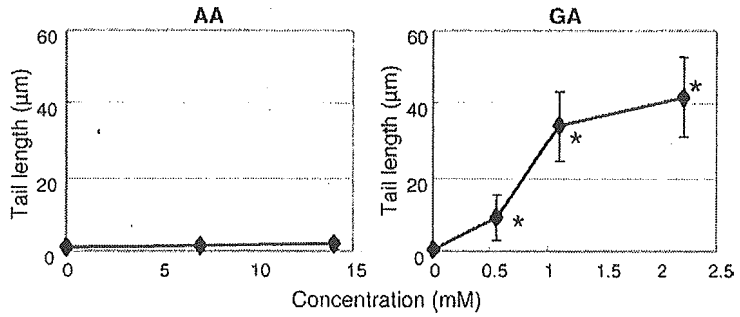

Fig. 2. COM assay results in TK6 cells treated with AA or GA for 4 h without metabolic activation. Asterisk (*) statistically significant in the Dunnett's tests ($P<0.05$).

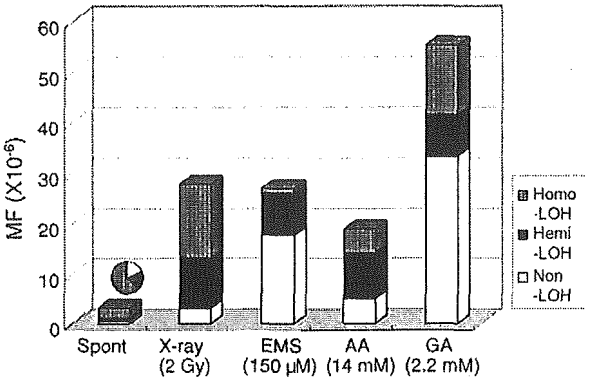

Fig. 3. Frequency and spectra of TK mutations in spontaneous and X-ray-induced (2 Gy), EMS-induced (150 μM, 4 h), AA-induced (14 mM, 4 h) and GA-induced (2.2 mM, 4 h) TK mutants in TK6 cells. The fraction of each mutational event was calculated by considering the ratio of normally growing (NG) and slowly growing (SG) mutants and the results of molecular analysis (Table 1). The data of spontaneous, X-ray-induced and EMS-induced mutation spectra were taken from our previous paper [13].

distribution of LOH in GA-induced and spontaneous LOH mutants was similar.

3.3. Cytotoxicity and genotoxicity of AA under metabolic activation

Rat liver S9 mix did not influence the cytotoxicity or genotoxicity of AA but it did enhance the activity of DBN, the positive control chemical (Fig. 5).

4. Discussion

A large number of studies about the in vitro genotoxicity of AA have been reported [8]. AA has consistently been negative in bacterial gene mutation assay in both the presence and absence of metabolic activation [23–25] but positive in chromosome aberration and sister chromatid exchange tests in Chinese hamster cell lines [24–26]. In mammalian cell assays, AA induces *Tk* but not *Hprt* gene mutations [24,25,27,28], and is negative in the COM assay even at high concentrations [27]. These results suggest that AA is clastogenic without directly damaging DNA. GA, on the other hand, is positive in most in vitro genotoxicity tests and is recognized as a mutagen [8,27,29]. In the present study, the higher concentrations of AA were positive in the MN and TK assay but negative in the comet assay. According to the in vitro genotoxicity test guideline, however, AA may be negative [30], because the guideline suggests that the maximum concentration should be 10 mM. Because the genotoxic responses at higher concentrations were reproducible, AA may be genotoxic, but its effect is very weak. GA, in contrast, was positive in all the assays, even under conditions of low cytotoxicity. These results are consistent with the reports described above.

The mammalian *TK* gene mutation assay can detect a wide range of genetic changes, including point mutations, small deletions, large-scale chromosomal deletions, inter-allelic recombination and aneuploidy, while

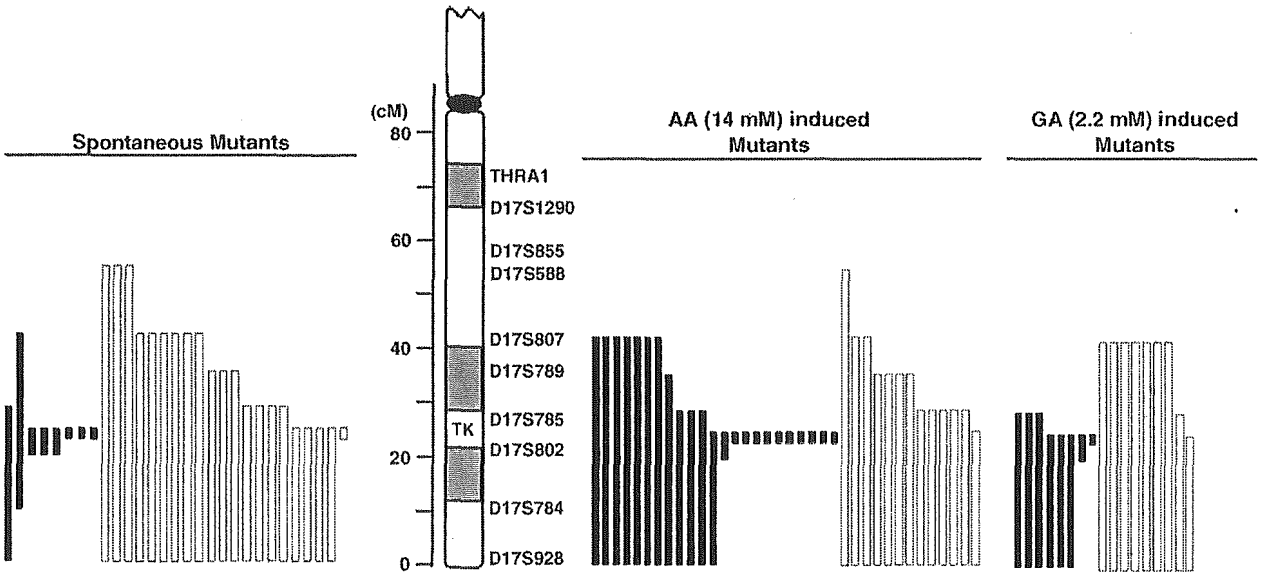

Fig. 4. The extent of LOH in spontaneous, AA-induced and GA-induced LOH mutants from TK6 cells. We examined 10 microsatellite loci on chromosome 17q that are heterozygous in TK6 cells. The human TK locus maps to 17q23.2. Open and closed bars represent homo-LOH and hemi-LOH, respectively. The length of the bar indicates the extent of the LOH. We analyzed 29 spontaneous mutants (10 NG and 19 SG mutants), 37 AA-induced mutants (11 NG and 26 SG) and 17 GA-induced mutants (2 NG and 15 SG). The data on spontaneous mutants were taken from our previous paper [13].

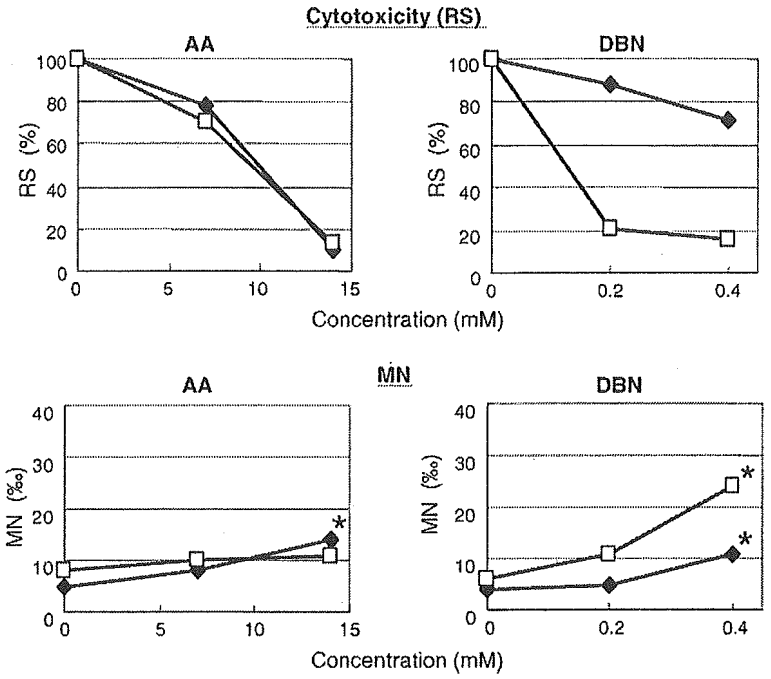

Fig. 5. Cytotoxicity (RS) and MN induction in TK6 cells treated with AA or DBN for 4 h in the presence (open symbol) or absence (closed symbol) of rat liver S9. Asterisk (*) statistically significant experiments in both pair-wise comparison and trend test ($P < 0.05$).

the bacterial and mammalian *HPRT* gene mutation assays detect only point mutations and small intragenic deletions [13]. AA was positive only in the *TK* mutation assay, suggesting that AA causes predominantly large-scale chromosomal changes. Our molecular analysis of the *TK* mutants supported this hypothesis. The majority of the AA-induced *TK* mutants showed hemi-LOH, which is the result of a deletion, although the other types were also induced (Fig. 3). Deletions are thought to result from the repair of double strand breaks by non-homlogous end-joining [13]. Radiation-induced double strand breaks are repaired by non-homlogous end-joining, which leads to hemi-LOH. LOH-mapping analysis, however, revealed that AA frequently induces intermediate-sized deletions (100–3000 kb); the deletions encompass exons 4 and 7 of the *TK* locus but do not extend to the microsatellites loci of the vicinity. This type of deletion is rarely observed in radiation-inducing *TK* mutants [13]. Because the COM assay indicated that AA did not induce DNA damage, the deletion may not be caused by DNA damage directly. Mechanisms associated with global genomic instability should also be considered [10] because the LOH patterns, except for the intermediate-sized deletions, are generally similar to those observed in spontaneous mutants. Most GA-induced *TK* mutants, on the other hand, were the non-LOH type, as were most spontaneous ones, strongly supporting the positive results in bacterial gene mutation assay [29]. In contrast to AA, GA is a mutagen, inducing primarily point mutations.

AA is known to be metabolized to GA by CYP2E1 [9]. GA, an epoxide, forms adducts directly with DNA and protein, causing cytotoxicity and genotoxicity. GA forms mainly *N*7-(2-carbamoyl-2-hydroxyethyl) guanine and *N*3-(2-carbamoyl-2-hydroxyethyl) adenine and reacts with hemoglobin and cytoskeletal proteins [31–33]. Rat S9, however, did not affect AA cytotoxicity or genotoxicity, although it did enhance the cytotoxicity and genotoxicity of DBN, which is also metabolized by CYP2E1. This suggests that rat S9 does not work for activating AA. AA and GA are detoxified through glutathione conjugation, and GA is also detoxified by epoxy hydrolase (EH), which catalyzes the hydrolysis of GA to dihidroxy propionamide [34,35]. Other in vitro studies also failed to demonstrate the enhancement of AA genotoxicity by rat S9 [36,37]. Our results do not mean that AA is always detoxified rather than activated because DNA adducts are found in mice and rats given oral AA, and the genotoxicity of AA is consistently observed in in vivo studies [8,31,36,37]. Recently, Manjanatha et al. demonstrated in transgenic Big Blue^{TM} mice that AA as well as GA induces endogenous *Hprt* and transgenic *cII* mutation at same level, and both chemicals cause predominantly base substitutions and frameshift mutations.

This result may indicate that AA is metabolized to GA in vivo [38]. Tests that use rat liver S9 for metabolic activation may not be appropriate for in vitro investigations of AA genotoxicity and metabolism. Transgenic cells expressing CYP2E1, however, would be useful for demonstrating the in vitro genotoxicity of AA [39].

In conclusion, AA is weakly genotoxic, causing chromosome aberrations and a type of genomic instability. GA, its epoxide metabolite, is highly reactive with DNA. GA is a strong mutagen, inducing predominantly point mutations, and it may contribute to human cancers.

Acknowledgment

This study was supported by Health and Labor Sciences Research Grants in Japan.

References

[1] IARC, Acrylamide, IARC Monographs on the Evaluation of Carcinogen Risk to Human: Some Industrial Chemicals, vol. 60, International Agency for Research on Cancer, Lyon, 1994, pp. 389–433.
[2] E. Tareke, P. Rydberg, P. Karlsson, S. Eriksson, M. Tornqvist, Acrylamide: a cooking carcinogen? Chem. Res. Toxicol. 13 (2000) 517–522.
[3] R.H. Stadler, I. Blank, N. Varga, F. Robert, J. Hau, P.A. Guy, M.C. Robert, S. Riediker, Acrylamide from Maillard reaction products, Nature 419 (2002) 449–450.
[4] d.S. Mottram, B.L. Wedzicha, A.T. Dodson, Acrylamide is formed in the Maillard reaction, Nature 419 (2002) 448–449.
[5] J.M. Rice, The carcinogenicity of acrylamide, Mutat. Res. 580 (2005) 3–20.
[6] E.J. Lehning, C.D. Balaban, J.F. Ross, M.A. Reid, R.M. LoPachin, Acrylamide neuropathy. I. Spatiotemporal characteristics of nerve cell damage in rat cerebellum, Neurotoxicology 23 (2002) 397–414.
[7] R.M. LoPachin, C.D. Balaban, J.F. Ross, Acrylamide axonopathy revisited, Toxicol. Appl. Pharmacol. 188 (2003) 135–153.
[8] K.L. Dearfield, G.R. Douglas, U.H. Ehling, M.M. Moore, G.A. Sega, D.J. Brusick, Acrylamide: a review of its genotoxicity and an assessment of heritable genetic risk, Mutat. Res. 330 (1995) 71–99.
[9] S.C. Sumner, T.R. Fennell, T.A. Moore, B. Chanas, F. Gonzalez, B.I. Ghanayem, Role of cytochrome P450 2E1 in the metabolism of acrylamide and acrylonitrile in mice, Chem. Res. Toxicol. 12 (1999) 1110–1116.
[10] M. Friedman, Chemistry, biochemistry, and safety of acrylamide. A review, J. Agric. Food Chem. 51 (2003) 4504–4526.
[11] H.M. Bolt, Genotoxicity–threshold or not? Introduction of cases of industrial chemicals, Toxicol. Lett. 140–141 (2003) 43–51.
[12] H.L. Liber, W.G. Thilly, Mutation assay at the thymidine kinase locus in diploid human lymphoblasts, Mutat. Res. 94 (1982) 467–485.
[13] M. Honma, Generation of loss of heterozygosity and its dependency on p53 status in human lymphoblastoid cells, Environ. Mol. Mutagen. 45 (2005) 162–176.
[14] M. Honma, M. Hayashi, T. Sofuni, Cytotoxic and mutagenic responses to X-rays and chemical mutagens in normal and p53-mutated human lymphoblastoid cells, Mutat. Res. 374 (1997) 89–98.
[15] K. Sekihashi, H. Saitoh, Y. Sasaki, Genotoxicity studies of stevia extract and steviol by the comet assay, J. Toxicol. Sci. 27 (Suppl. 1) (2002) 1–8.
[16] M. Watanabe-Akanuma, T. Ohta, Y.F. Sasaki, A novel aspect of thiabendasole as a photomutagen in bacteria and cultured human cells, Mutat. Res. 158 (2005) 213–219.
[17] L. Zhan, H. Sakamoto, M. Sakuraba, D.S. Wu, L.S. Zhang, T. Suzuki, M. Hayashi, M. Honma, Genotoxicity of microcystin-LR in human lymphoblastoid TK6 cells, Mutat. Res. 557 (2004) 1–6.
[18] T. Matsushima, M. Hayashi, A. Matsuoka, M. Ishidate Jr., K.F. Miura, H. Shimizu, Y. Suzuki, K. Morimoto, H. Ogura, K. Mure, K. Koshi, T. Sofuni, Validation study of the in vitro micronuclei test in a Chinese hamuster lung cell line (CHL/IU), Mutagenesis 14 (1999) 569–580.
[19] S.A. Amundson, H.L. Liber, A comparison of induced mutation at homologous alleles of the tk locus in human cells, Mutat. Res. 247 (1991) 19–27.
[20] E.E. Furth, W.G. Thilly, B.W. Penman, H.L. Liber, W.M. Rand, Quantitative assay for mutation in diploid human lymphoblasts using microtiter plates, Anal. Biochem. 110 (1981) 1–8.
[21] T. Omori, M. Honma, M. Hayashi, Y. Honda, I. Yoshimura, A new statistical method for evaluating of L5178Ytk± mammalian cell data using microwell method, Mutat. Res. 517 (2002) 199–208.
[22] M. Honma, M. Momose, H. Tanabe, H. Sakamoto, Y. Yu, J.B. Little, T. Sofuni, M. Hayashi, Requirement of wild-type p53 protein for maintenance of chromosomal integrity, Mol. Carcinog. 28 (2000) 203–214.
[23] E. Zeiger, B. Anderson, S. Haworth, T. Lawlor, K. Mortelmans, W. Speck, Salmonella mutagenicity tests: III. Results from the testing of 255 chemicals, Environ. Mutagen. 9 (Suppl. 9) (1987) 1–109.
[24] H. Tsuda, C.S. Shimizu, M.K. Taketomi, M.M. Hasegawa, A. Hamada, K.M. Kawata, N. Inui, Acrylamide; induction of DNA damage, chromosomal aberrations and cell transformation without gene mutations, Mutagenesis 8 (1993) 23–29.
[25] A.G. Knaap, P.G. Kramers, C.E. Voogd, W.G. Bergkamp, M.G. Groot, P.G. Langebroek, H.C. Mout, J.J. van der Stel, H.W. Verharen, Mutagenic activity of acrylamide in eukaryotic systems but not in bacteria, Mutagenesis 3 (1988) 263–268.
[26] T. Sofuni, M. Hayashi, A. Matsuoka, M. Sawada, Mutagenicity tests on organic chemical concominants in city water and related compounds. II. Chromosome aberration tests in cultured mammalian cells, Eisei Shiken. Hok. 103 (1985) 64–75.
[27] M. Baum, E. Fauth, S. Fritzen, A. Herrmann, P. Mertes, K. Merz, M. Rudolphi, H. Zankl, G. Eisenbrand, Acrylamide and glycidamide: genotoxic effects in V79-cells and human blood, Mutat. Res. 580 (2005) 61–69.
[28] M.M. Moore, A. Amtower, C. Doerr, K.H. Brock, K.L. Dearfield, Mutagenicity and clastogenicity of acrylamide in L5178Y mouse lymphoma cells, Environ. Mutagen. 9 (1987) 261–267.
[29] K. Hashimoto, H. Tanii, Mutagenicity of acrylamide and its analogues in *Salmonella typhimurium*, Mutat. Res. 158 (1985) 129–133.
[30] C.S. Aaron, G. Bolcsfoldi, H.R. Glatt, M. Moore, Y. Nishi, L. Stankowski, Theiss F J., E. Thompson, Mammalian cell gene mutation assays working group report, Mutat Res. 312 (1994) 235–239.

[31] d.C. Gamboa, M.I. Churchwell, L.P. Hamilton, L.S. Von Tungeln, F.A. Beland, M.M. Marques, D.R. Doerge, DNA adduct formation from acrylamide via conversion to glycidamide in adult and neonatal mice, Chem. Res. Toxicol. 16 (2003) 1328–1337.
[32] D.M. Lapadula, M. Bowe, C.D. Carrington, L. Dulak, M. Friedman, M.B. Abou-Donia, In vitro binding of [14C]acrylamide to neurofilament and microtubule proteins of rats, Brain Res. 481 (1989) 157–161.
[33] S.C. Sumner, C.C. Williams, R.W. Snyder, W.L. Krol, B. Asgharian, T.R. Fennell, Acrylamide: a comparison of metabolism and hemoglobin adducts in rodents following dermal, intraperitoneal, oral, or inhalation exposure, Toxicol. Sci. 75 (2003) 260–270.
[34] B. Paulsson, A. Rannug, A.P. Henderson, B.T. Golding, M. Tornqvist, M. Warholm, In vitro studies of the influence of glutathione transferases and epoxide hydrolase on the detoxification of acrylamide and glycidamide in blood, Mutat. Res. 580 (2005) 53–59.
[35] S.C. Sumner, L. Selvaraj, S.K. Nauhaus, T.R. Fennell, Urinary metabolites from F344 rats and B6C3F1 mice coadministered acrylamide and acrylonitrile for 1 or 5 days, Chem. Res. Toxicol. 10 (1997) 1152–1160.
[36] A. Besaratinia, G.P. Pfeifer, Genotoxicity of acrylamide and glycidamide, J. Natl. Cancer Inst. 96 (2004) 1023–1029.
[37] A. Besaratinia, G.P. Pfeifer, DNA adduction and mutagenic properties of acrylamide, Mutat. Res. 580 (2005) 31–40.
[38] M.G. Manjanatha, A. Aidoo, S.D. Shelton, M.E. Bishop, L.P. MacDaniel, D.R. Doerge, Genotoxicity of acrylamide and its metabolite glycidamide administrated in drinking water to male and female Big Blue mice, Environ. Mol. Mutagen, in press (Epub ahead of prints).
[39] H. Glatt, H. Schneider, Y. Liu, V79-hCYP2E1-hSULT1A1, a cell line for the sensitive detection of genotoxic effects induced by carbohydrate pyrolysis products and other food-borne chemicals, Mutat. Res. 580 (2005) 41–52.

Available online at www.sciencedirect.com
SCIENCE DIRECT®
Biochimica et Biophysica Acta 1688 (2004) 137–144
BIOCHIMICA ET BIOPHYSICA ACTA
BBA
www.bba-direct.com

The absence of a functional relationship between ATM and BLM, the components of BASC, in DT40 cells

Wensheng Wang[a,b,1], Masayuki Seki[a,*], Makoto Otsuki[a], Shusuke Tada[a], Noriaki Takao[c], Ken-ichi Yamamoto[c], Makoto Hayashi[b], Masamitsu Honma[b], Takemi Enomoto[a]

[a] *Molecular Cell Biology Laboratory, Graduate School of Pharmaceutical Sciences, Tohoku University, Sendai 980-8578, Japan*
[b] *Division of Genetics and Mutagenesis, National Institute of Health Sciences, 1-18-1, Kamiyoga, Setagaya, Tokyo 158-8501, Japan*
[c] *Department of Molecular Pathology, Cancer Research Institute, Kanazawa University, Kanazawa 920-0934, Japan*

Received 3 May 2002; received in revised form 11 November 2003; accepted 12 November 2003

Abstract

Bloom syndrome (BS) and ataxia-telangiectasia (A-T) are rare autosomal recessive diseases associated with chromosomal instability. The genes responsible for BS and A-T have been identified as *BLM* and *ATM*, respectively, whose products were recently found to be components of BRCA1-associated genome surveillance complex (BASC), a supercomplex possibly involved in the recognition and repair of aberrant DNA structures. Based on experiments using $BLM^{-/-}$ DT40 cells and $BLM^{-/-}/RAD54^{-/-}$ DT40 cells, we previously suggested that BLM functions to reduce the formation of double-strand breaks (DSBs) during DNA replication. To examine whether ATM is involved in the recognition and/or repair of DSBs generated in $BLM^{-/-}$ DT40 cells and to address the functional relationship between the two BASC components, we generated $BLM^{-/-}/ATM^{-/-}$ DT40 cells and characterized their properties as well as those of $ATM^{-/-}$ and $BLM^{-/-}$ DT40 cells. $BLM^{-/-}/ATM^{-/-}$ cells proliferated slightly more slowly than either $BLM^{-/-}$ or $ATM^{-/-}$ cells. The sensitivity of $BLM^{-/-}/ATM^{-/-}$ cells to γ-irradiation was similar to that of $ATM^{-/-}$ cells, while $BLM^{-/-}$ cells were slightly resistant to γ-irradiation compared with wild-type cells. $BLM^{-/-}$ cells showed sensitivity to methyl methanesulfonate (MMS) and UV irradiation while $ATM^{-/-}$ cells did not show sensitivity to either agent. The sensitivity of $BLM^{-/-}/ATM^{-/-}$ cells to MMS and UV was similar to that of $BLM^{-/-}$ cells. Disrupting the function of ATM reduced the targeted integration frequency in $BLM^{-/-}$ DT40 cells. However, a defect in ATM only slightly reduced the increased sister chromatid exchanges (SCEs) in $BLM^{-/-}$ DT40 cells.

Keywords: BLM; ATM; BASC; Targeted integration; SCE; DSB

1. Introduction

Bloom syndrome (BS) is a rare autosomal recessive disease characterized by immunodeficiency, retarded growth, male sterility, sensitivity to sunlight, and a predisposition to a wide variety of cancers. Cells derived from BS patients exhibit elevated frequencies of sister chromatid exchanges (SCEs), chromosomal breaks, and interchanges between homologous chromosomes [1]. However, they show a retarded rate of elongation of nascent DNA chains [2] and accumulate abnormal replication intermediates [3]. In addition, immunodepletion of *Xenopus* Bloom syndrome gene product (xBLM) from a *Xenopus* egg extract severely inhibited the replication of chromosomal DNA in reconstituted nuclei and the inhibition was cancelled by the addition of recombinant xBLM [4]. Thus, BLM seems to be somehow involved in DNA replication.

Ataxia-telangiectasia (A-T) is also a rare autosomal recessive disease displaying chromosome instability. Symptoms of A-T include cerebella ataxia, oculocutaneous telangiectasia, immunodeficiency, premature aging, predisposition to lymphoid malignancy, and radiosensitivity. Cells derived from A-T patients show high levels of chromosome aberrations and hypersensitivity to ionizing radiation [5]. The product of the gene responsible for A-T, ATM, is a member of the family of phosphoinositide kinases [6]. ATM plays essential roles in the recognition, signaling and repair of DNA damage, especially DNA double-strand breaks (DSBs). ATM is an upstream factor of p53 and

* Corresponding author. Tel.: +81-22-217-6874; fax: +81-22-217-6873.
E-mail address: seki@mail.pharm.tohoku.ac.jp (M. Seki).
[1] Present address: Department of Biochemistry and Biophysics, University of Rochester Medical Center, Rochester, NY 14642, USA.

0925-4439/$ - see front matter © 2003 Elsevier B.V. All rights reserved.
doi:10.1016/j.bbadis.2003.11.008

regulates progression of the cell-cycle and apoptosis by phosphorylating p53 [7,8]. ATM also interacts with and phosphorylates c-Abl, which interacts with p53, induces apoptosis and arrests cells in G1 phase after ionizing radiation [9,10]. Chk2 is also phosphorylated by ATM and regulates progression of the cell cycle through p53-dependent and independent pathways [11–13].

Recently, BLM and ATM have been reported to be components of BRCA1-associated genome surveillance complex (BASC), a supercomplex supposed to be involved in the recognition and repair of aberrant DNA structures, which consists of BRCA1, MSH2, MSH6, MLH1, RFCs, and RAD50 as well as BLM and ATM [14]. In addition, BLM is phosphorylated by ATM in response to ionizing radiation [15]. However, the functional relationship between BLM and the other components of BASC is not clear at present.

It has been reported that DSBs are produced by cleavage of the Holliday junctions which are formed by the annealing of two newly synthesized DNA at arrested replication forks [16]. The gene responsible for BS encodes a protein which is a member of the RecQ helicase family and actually has DNA helicase activity [17,18]. In addition, BLM selectively binds and acts on Holliday junctions to promote branch migration over an extended length of DNA [19]. In our previous study using *BLM*$^{-/-}$ cells constructed from a chicken B cell line, DT40 and *BLM*$^{-/-}$/*RAD54*$^{-/-}$ DT40

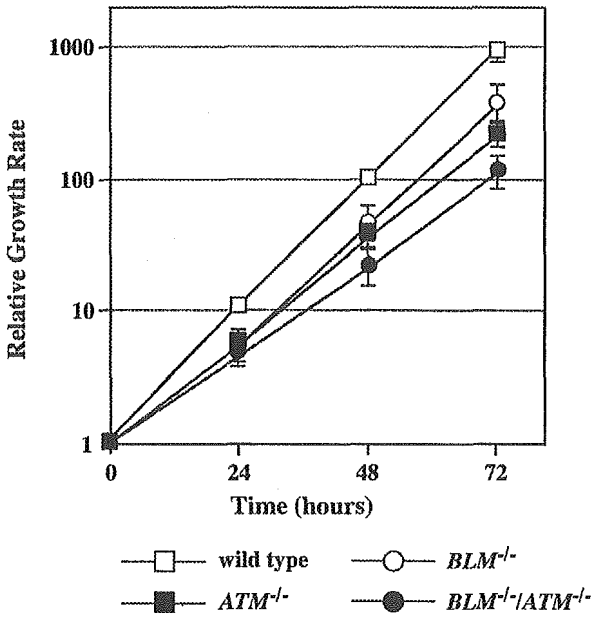

Fig. 2. Growth curves of wild-type, *ATM*$^{-/-}$, *BLM*$^{-/-}$ and *BLM*$^{-/-}$/*ATM*$^{-/-}$ DT40 cells. Wild-type, *ATM*$^{-/-}$, *BLM*$^{-/-}$ and *BLM*$^{-/-}$/*ATM*$^{-/-}$ DT40 cells were inoculated into 35 mm dishes, and enumerated at the time indicated. Three independent experiments were performed and typical data were presented. Error bars show the standard deviation of the mean.

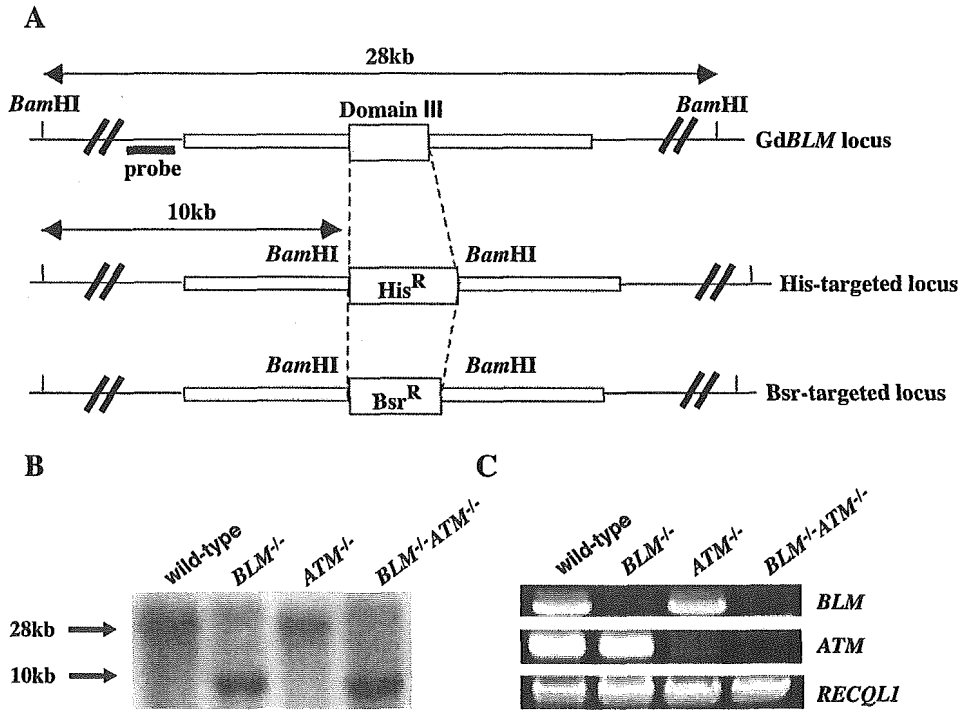

Fig. 1. Generation of DT40 *BLM*$^{-/-}$/*ATM*$^{-/-}$ double mutant cells. (A) Schematic representation of part of the *BLM* genomic locus, targeting constructs, and the configuration of the targeted locus. (B) Southern blot analyses for wild-type (+/+), *BLM*$^{-/-}$, *ATM*$^{-/-}$, and *BLM*$^{-/-}$/*ATM*$^{-/-}$ cells were carried out to confirm the *BLM* gene disruption in putative *BLM*$^{-/-}$/*ATM*$^{-/-}$ cells. *Bam*HI-digested genomic DNA was hybridized with the probe shown in panel A. (C) RT-PCR analysis of total RNA from wild-type (+/+), *BLM*$^{-/-}$, *ATM*$^{-/-}$, and *BLM*$^{-/-}$/*ATM*$^{-/-}$ cells. The primer sets used to detect *ATM*, *BLM*, and *RECQL1* (control) were described in Materials and methods.

cells, we suggested that the physiological function of BLM is to resolve Holliday junctions formed during DNA replication, and DSBs formed due to a defect in BLM function are repaired mainly by homologous recombination, resulting in an increased incidence of SCE [20]. However, the precise mechanism of the formation of SCE is not known. Interestingly, most of the components of BASC, such as BRCA1, MSH2, RAD50, and ATM, are known to be somehow involved in homologous recombination [14].

In this study, to examine whether ATM is involved in the formation of SCE in *BLM*$^{-/-}$ DT40 cells and to elucidate the functional relationship between the two BASC components, BLM and ATM, under DNA damage-induced conditions, we generated *BLM*$^{-/-}$/*ATM*$^{-/-}$ double gene-disrupted DT40 cells and characterized their properties as well as those of *BLM*$^{-/-}$ and *ATM*$^{-/-}$ DT40 cells.

2. Materials and methods

2.1. Construction of targeting vectors

Chicken *BLM*-targeting constructs, *BLM*-histidinol® and *BLM*-blasticidin S®, were made as described previously [20].

2.2. Cell culture and DNA transfection

The cell culture conditions were described previously [20]. *BLM*$^{-/-}$ and *ATM*$^{-/-}$ DT40 cells were generated as reported elsewhere [20,21]. To generate *BLM*$^{-/-}$/*ATM*$^{-/-}$ DT40 cells, *ATM*$^{-/-}$ DT40 cells were electroporated with 30 μg of linearized *BLM*-targeting constructs using a Gene Pulser II apparatus (BioRad, Hercules, CA, USA) at 550 V and 25 μF. Drug-resistant colonies were selected in 96-well plates with medium containing 1 mg/ml of histidinol or 20 μg/ml of blasticidin S. Gene disruption was confirmed by Southern blotting and RT-PCR. Primer sets used to detect *ATM*, *BLM*, and *RECQL1* (control) by RT-PCR are as follows:

ATM-sense:5′-GTGGATCCCACAGGAAGATA-3′
ATM-antisense: 5′-GTCAGCTTCATCCTCTGGTC-3′
BLM-sense: 5′-ACCAGCGTGTGTCTCTGCTG-3′
BLM-antisense: 5′-CTACAGATTTTGGAAGGGAAGC-3′
RECQL1-sense: 5′-ATGACAGCTGTGGAAGTGCTA-3′
RECQL1-antisense: 5′-TCAGTCAAGAACAA-CAGGTTGGTCATCTC-3′.

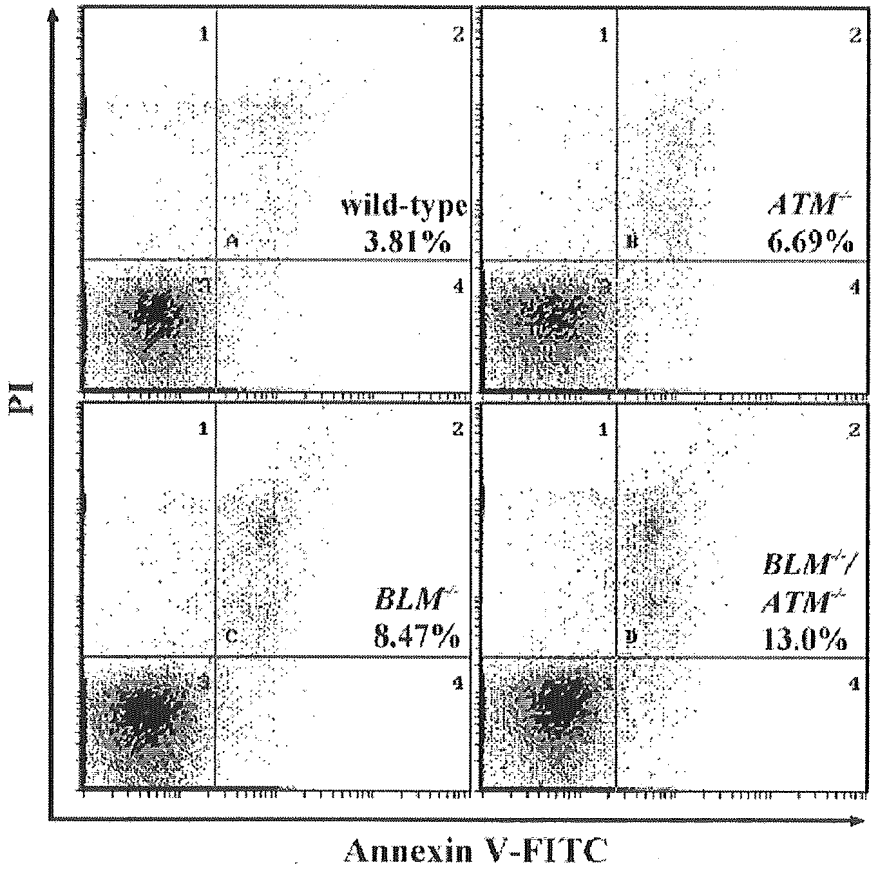

Fig. 3. Flow cytometry for detection of dead cells. Cells (5×10^5) were treated according to the Manual of the ApoAlert Annexin V-FITC Apoptosis kit and 3×10^4 cells were analyzed by Flow Cytometry. The number in the upper right corner indicates the percentage of dead cells.

2.3. Growth curve and flow cytometry

Cells (2×10^4) were inoculated and cultured at 39 °C for specified periods. They were then enumerated with a Particle Count and Size Analyzer (Coulter, USA) and relative growth rates were estimated. The cell cycle distribution pattern and cell death were examined with a EPICS XL Flow Cytometer (Coulter) after treatment according to the manual of the BrdU Flow Kit (Beckon Dickinson, CA) and ApoAlert Annexin V-FITC Apoptosis Kit (Clontech Laboratories, Inc., CA).

2.4. Measurements of MMS, UV and γ-radiation sensitivity

The sensitivity to methyl methanesulfonate (MMS) was evaluated as described previously [20]. To determine the sensitivity to UV or ionizing radiation, cells were irradiated with UV light or γ-rays at given doses, and then inoculated into dishes containing growth medium supplemented with 1.5% methylcellulose. The colonies were enumerated 9 days after inoculation. Survival was determined by comparing results with the number of colonies of untreated cells.

2.5. Measurements of targeted integration frequency and SCE frequency

To analyze targeted integration events at the chicken RECQL1, RECQL5 and RAD54 loci, a targeting construct, either chicken RECQL1-Hygromycin®, RECQL5-Hygromycin® or RAD54-Hygromycin® (a gift from Dr. Takeda), was transfected into cells, and then cells were selected with the medium containing 2.5 mg/ml of hygromycin (Wako Pure Chemical Industries, Ltd. Japan). Genomic DNA of drug-resistant clones was isolated and targeted integration was confirmed by polymerase chain reaction and Southern blotting. SCE analysis was performed as described previously [22].

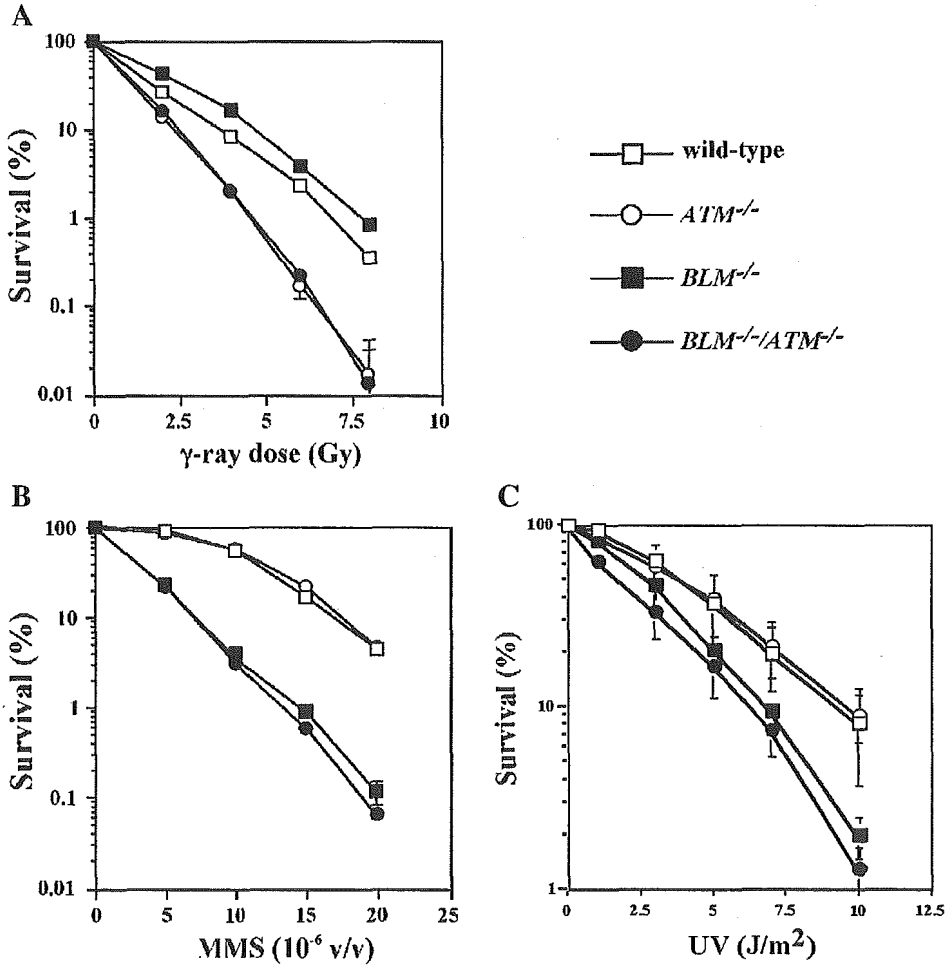

Fig. 4. Sensitivity of cells with various genotypes to γ-irradiation, MMS, and UV-irradiation. (A) γ-irradiation sensitivity, (B) MMS sensitivity, (C) UV-irradiation sensitivity. Sensitivities of wild-type, $ATM^{-/-}$, $BLM^{-/-}$, and $BLM^{-/-}/ATM^{-/-}$ DT40 cells to γ-irradiation, MMS, and UV-irradiation were determined as described under Materials and methods. Three independent experiments were performed and typical data were presented. Each value represents the mean of the survival rate and error bars show the standard deviation of the mean.

3. Results

To generate $ATM^{-/-}/BLM^{-/-}$ DT40 cells, *BLM*-histidinol® and *BLM*-blasticidin S® targeting vectors were sequentially transfected into $ATM^{-/-}$ DT40 cells (Fig. 1A) [21]. Disruption of the corresponding genes in $ATM^{-/-}/BLM^{-/-}$, $BLM^{-/-}$, and $ATM^{-/-}$ cells was confirmed by Southern blotting (Fig. 1B). In addition, we confirmed by RT-PCR the absence of *ATM* message in $ATM^{-/-}$ cells and $BLM^{-/-}/ATM^{-/-}$ cells, and the absence of *BLM* message in $BLM^{-/-}$ cells and $BLM^{-/-}/ATM^{-/-}$ cells (Fig. 1C).

We first monitored the growth curves of wild-type, $ATM^{-/-}$, $BLM^{-/-}$ and $BLM^{-/-}/ATM^{-/-}$ cells. $BLM^{-/-}/ATM^{-/-}$ cells proliferated at a lower rate than either single mutant indicating that the simultaneous defect of ATM and BLM results in an additive effect on cell proliferation (Fig. 2). To obtain an insight into the cause of the slow growth phenotype in $BLM^{-/-}/ATM^{-/-}$ DT40 cells, we investigated cell cycle distribution patterns and spontaneous cell death by flow cytometry. $BLM^{-/-}/ATM^{-/-}$ cells showed no obvious difference in cell cycle distribution (data not shown), but they showed a high rate of spontaneous cell death as compared with $ATM^{-/-}$, $BLM^{-/-}$, or wild-type cells (Fig. 3).

It has been demonstrated that ATM-deficient DT40 cells exhibit high sensitivity to ionizing irradiation [20,21]. Thus, we examined the sensitivity to γ-irradiation of $BLM^{-/-}/ATM^{-/-}$ cells as well as wild-type, $ATM^{-/-}$, and $BLM^{-/-}$ cells. As shown in Fig. 4A, the sensitivity of $BLM^{-/-}/ATM^{-/-}$ cells to γ-irradiation was similar to that of $ATM^{-/-}$ cells. In contrast to $ATM^{-/-}$ cells, $BLM^{-/-}$ cells were slightly resistant to γ-irradiation as compared with wild-type cells.

We previously reported that $BLM^{-/-}$ DT40 cells showed hypersensitivity to MMS as compared with wild-type cells [20]. Thus, we next investigated the sensitivity of $ATM^{-/-}/BLM^{-/-}$ cells to MMS. In contrast to $BLM^{-/-}$ cells, $ATM^{-/-}$ cells showed a similar sensitivity to MMS as the wild-type cells. The sensitivity of $ATM^{-/-}/BLM^{-/-}$ cells to MMS was similar to that of $BLM^{-/-}$ cells (Fig. 4B). Similar results were obtained upon exposure to ultraviolet light (Fig. 4C).

Table 1
Targeted integration frequency

Locus[a]	Targeted integration/total integration (%)			
	Wild-type	$ATM^{-/-}$	$BLM^{-/-}$	$BLM^{-/-}/ATM^{-/-}$
RECQL1	41.67 ± 0.00	37.50 ± 5.89	87.50 ± 5.89	66.67 ± 3.61*
RECQL5	37.50 ± 5.89	27.08 ± 2.95	83.33 ± 2.95	54.17 ± 7.22*
RAD54	45.83 ± 5.89	25.00 ± 0.00	95.83 ± 0.00	68.14 ± 5.01**

[a] Indicated loci were targeted by targeting constructs *RECQL1*-Hygromycin®, *RECQL5*-Hygromycin®, and *RAD54*-Hygromycin®. Results are represented as means ± S.D. of two to three experiments. Significant differences from the value of $BLM^{-/-}$ are represented by * ($P<0.05$) or ** ($P<0.01$). Statistical analysis was performed by means of Student's *t*-test.

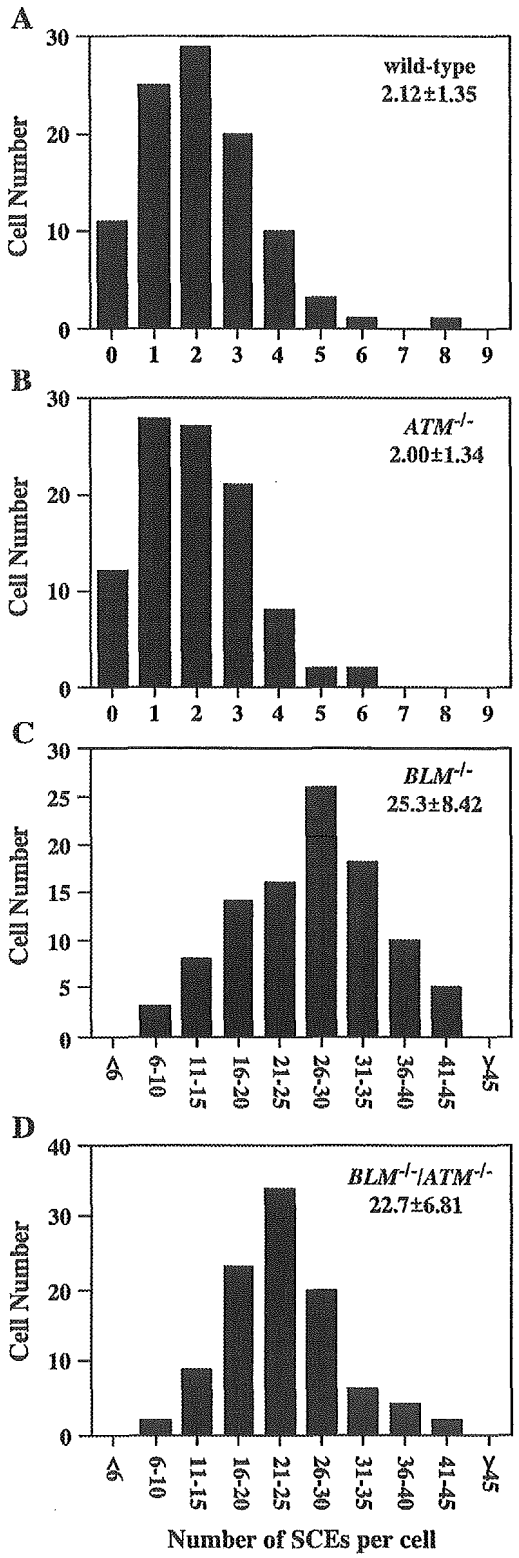

Fig. 5. Histograms of SCE in cells with various genotypes. Spontaneous SCEs in the macrosomes of 100 metaphase cells were counted. Histograms show the frequency of cells with the indicated number of SCEs per cell. The mean ± S.D. number of SCEs per cell is shown in the upper right corner.

BLM$^{-/-}$ DT40 cells showed an increased incidence of SCE and increased targeted integration frequency [20]. Thus, it is interesting to examine whether ATM is involved in the targeted integration and SCE in *BLM*$^{-/-}$ cells. As shown in Table 1, *ATM*$^{-/-}$ cells showed a slightly lower targeted integration frequency than wild-type cells as described previously [21]. The targeted integration frequencies in *BLM*$^{-/-}$/*ATM*$^{-/-}$ cells were higher than those in wild-type cells, but lower than those in *BLM*$^{-/-}$ cells, indicating that ATM is partly involved in targeted integration in *BLM*$^{-/-}$ DT40 cells.

We next analyzed frequencies of SCE in wild-type, *ATM*$^{-/-}$, *BLM*$^{-/-}$, and *BLM*$^{-/-}$/*ATM*$^{-/-}$ cells. The frequency of SCE in *ATM*$^{-/-}$ cells was almost the same as that in wild-type cells (Fig. 5A and B). The increased frequency of SCE in *BLM*$^{-/-}$ cells was only slightly decreased by the disruption of the *ATM* gene ($P<0.05$) (Fig. 5C and D), indicating a small contribution of ATM to the formation of SCE in *BLM*$^{-/-}$ DT40 cells.

4. Discussion

To our knowledge, this is the first study to genetically investigate the functional relationship between BLM and ATM, two of the components of BASC. It has been demonstrated that BLM is phosphorylated by ATM in response to ionizing radiation [15]. The sensitivity of *ATM*$^{-/-}$/*BLM*$^{-/-}$ cells to γ-irradiation was similar to that of *ATM*$^{-/-}$ cells, and *BLM*$^{-/-}$ cells showed slight resistance to γ-irradiation compared with wild-type cells. The results indicate that ATM plays an important role in the repair of DNA lesions induced by γ-irradiation as expected, while BLM has essentially no function in the repair of these lesions at least when the function is assessed based on viability. ATM is thought to be a signaling protein acting in response to DNA damage induced by ionizing radiation as a sensor. Suzuki et al. [23] have demonstrated that ATM associates with double strand DNA and the association is increased under ionizing radiation. In addition, after ionizing radiation, ATM phosphorylates the downstream proteins that are involved in DNA recombination repair [24]. In contrast, BLM is not thought to be involved directly in DNA recombination repair. Consistent with this notion, it has been indicated that a defect of BLM does not affect the formation of RAD51 foci under ionizing radiation [25,26]. Taken together, these result further support the notion that BLM functions to reduce the formation of DSBs during DNA replication [20] and is not involved in the repair of DSBs.

The slight resistance of *BLM*$^{-/-}$ cells to γ-irradiation is reminiscent of the observation that cells exposed to low-dose ionizing radiation or hydrogen peroxide are less sensitive to high-dose ionizing radiation [27]. Our previous studies suggest that slightly more DNA lesions occur when there is a defect in BLM. Thus it seems likely that the slight resistance of *BLM*$^{-/-}$ cells to γ-irradiation is caused by the activation of the DSB repair system due to an increase in DSBs in *BLM*$^{-/-}$ cells under conditions not inducing damage.

Methyl methanesulfonate (MMS) causes the methylation of DNA bases, and a methylated base such as 3-methyladenine is thought to block DNA replication [28]. Recent studies using prokaryotic and eukaryotic cells indicated that the Holliday junctions are formed at arrested replication forks [16,29], and the cleavage of such junctions leads to the formation of DSBs at arrested replication forks [16]. We previously suggested that the physiological function of BLM is to resolve Holliday junctions. If this is the case, the number of DSBs will be considerably increased upon exposure to MMS in BLM-defective cells. However, the sensitivity of *ATM*$^{-/-}$/*BLM*$^{-/-}$ DT40 cells to MMS was similar to that of *BLM*$^{-/-}$ DT40 cells, indicating that ATM is not essential to the repair of DSBs formed in *BLM*$^{-/-}$ cells on exposure to MMS.

The defect of ATM only slightly reduced the increased SCE in *BLM*$^{-/-}$ DT40 cells, indicating a minor contribution of ATM to the formation of SCE in *BLM*$^{-/-}$ DT40 cells. We previously suggested that the defect of BLM causes the formation of DSBs during DNA replication, and these DSBs are repaired mainly by homologous recombination, resulting in an increased incidence of SCE [20]. Thus, the small contribution of ATM to the formation of SCE in *BLM*$^{-/-}$ DT40 is not surprising because DNA lesions formed during DNA replication could be recognized by ATR instead of ATM.

It has been reported that p53 binds to BLM in vivo and in vitro and localizes at stalled DNA replication sites depending on BLM [30]. In addition, the depletion of p53 in the cells derived from a Bloom syndrome individual slightly increased the frequency of SCE. Thus, it is interesting to analyze the functional relationship between BLM and p53. However, DT40 cells do not express p53 [21], and the phenotypes of *ATM*$^{-/-}$, *BLM*$^{-/-}$, and *ATM*$^{-/-}$/*BLM*$^{-/-}$ DT40 cells represent those of these cells in the absence of p53. It seems likely that the increase in the frequency of SCE in *BLM*$^{-/-}$ and *ATM*$^{-/-}$/*BLM*$^{-/-}$ DT40 cells involves the contribution of the defects in both BLM and p53 although the contribution of p53 is small.

It has been reported that a defect of ATM causes the slower accumulation of RAD51 foci in response to ionizing radiation [31], and ATM phosphorylates BRCA1, NBS1 and Rad51 [32–35]. In addition, a defect in BRCA1 reduces homologous recombination [36]. These results indicate that ATM is somehow involved in homologous recombination. The defect of ATM partially reduced the increased targeted integration frequency in *BLM*$^{-/-}$ DT40 cells, indicating the involvement of ATM in homologous recombination. It seems likely that in the case of targeted integration, there exist double strand DNA ends of transfected DNA regardless of DNA replication and these double strand DNA ends are recognized by ATM.

In summary, although BLM is phosphorylated by ATM in response to ionizing radiation [15], and BLM and ATM are components of BASC [14], we could find little functional relationship between BLM and ATM. While circumstantial evidence strongly indicates the formation of DSBs in *BLM*$^{-/-}$ DT40 cells under MMS-exposed and non-exposed conditions, the contribution of ATM to the repair of DSBs formed in *BLM*$^{-/-}$ DT40 cells, seems to be very small. We speculate that the DSBs that are formed during DNA replication in the absence of BLM are specifically channeled to a homologous recombination pathway via components of BASC other than ATM, such as BRCA1 and RAD50/MRE11/NBS1. The identification of such channeling factors among the components of BASC will shed light on the function of BASC.

Acknowledgements

We thank Dr. Takeda for kindly providing the *RAD54*-Hygromycin® vector. This work was supported by Grants-in-Aid for Scientific Research from the Ministry of Education, Culture, Science, Sports, and Technology of Japan, a Health Sciences Research Grant from the Ministry of Health, Labor, and Welfare of Japan, and a grant from the Uehara Memorial Foundation. M. Seki was supported in part by the Mochida Memorial Foundation for Medical and Pharmaceutical Research.

References

[1] J. German, Bloom syndrome: a mendelian prototype of somatic mutational disease, Medicine (Baltimore) 72 (1993) 393–406.
[2] R. Hand, J. German, A retarded rate of DNA chain growth in Bloom's syndrome, Proc. Natl. Acad. Sci. U. S. A. 72 (1975) 758–762.
[3] U. Lonn, S. Lonn, U. Nylen, G. Winblad, J. German, An abnormal profile of DNA replication intermediates in Bloom's syndrome, Cancer Res. 50 (1990) 3141–3145.
[4] S. Liao, J. Graham, H. Yan, The function of *Xenopus* Bloom's syndrome protein homolog (xBLM) in DNA replication, Genes Dev. 14 (2000) 2570–2575.
[5] M.C. Paterson, P.J. Smith, Ataxia telangiectasia: an inherited human disorder involving hypersensitivity to ionizing radiation and related DNA-damaging chemicals, Annu. Rev. Genet. 13 (1979) 291–318.
[6] K. Savitsky, A. Bar-Shira, S. Gilad, G. Rotman, Y. Ziv, L. Vanagaite, D.A. Tagle, S. Smith, T. Uziel, S. Sfez, A single ataxia telangiectasia gene with a product similar to PI-3 kinase, Science 268 (1995) 1749–1753.
[7] C.E. Canman, D.S. Lim, K.A. Cimprich, Y. Taya, K. Tamai, K. Sakaguchi, E. Appella, M.B. Kastan, J.D. Siliciano, Activation of the ATM kinase by ionizing radiation and phosphorylation of p53, Science 281 (1998) 1677–1679.
[8] S. Banin, L. Moyal, S. Shieh, Y. Taya, C.W. Anderson, L. Chessa, N.I. Smorodinsky, C. Prives, Y. Reiss, Y. Shiloh, Y. Ziv, Enhanced phosphorylation of p53 by ATM in response to DNA damage, Science 281 (1998) 1674–1677.
[9] R. Baskaran, L.D. Wood, L.L. Whitaker, C.E. Canman, S.E. Morgan, Y. Xu, C. Barlow, D. Baltimore, A. Wynshaw-Boris, M.B. Kastan, J.Y. Wang, Ataxia telangiectasia mutant protein activates c-Abl tyrosine kinase in response to ionizing radiation, Nature 387 (1997) 516–519.
[10] T. Shafman, K.K. Khanna, P. Kedar, K. Spring, S. Kozlov, T. Yen, K. Hobson, M. Gatei, N. Zhang, D. Watters, M. Egerton, Y. Shiloh, S. Kharbanda, D. Kufe, M.F. Lavin, Interaction between ATM protein and c-Abl in response to DNA damage, Nature 387 (1997) 520–523.
[11] S. Matsuoka, M. Huang, S.J. Elledge, Linkage of ATM to cell cycle regulation by the Chk2 protein kinase, Science 282 (1998) 1893–1897.
[12] K. Tominaga, H. Morisaki, Y. Kaneko, A. Fujimoto, T. Tanaka, M. Ohtsubo, M. Hirai, H. Okayama, K. Ikeda, M. Nakanishi, Role of human Cds1 (Chk2) kinase in DNA damage checkpoint and its regulation by p53, J. Biol. Chem. 274 (1999) 31463–31467.
[13] N.H. Chehab, A. Malikzay, M. Appel, T.D. Halazonetis, Chk2/hCds1 functions as a DNA damage checkpoint in G(1) by stabilizing p53, Genes Dev. 14 (2000) 278–288.
[14] Y. Wang, D. Cortez, P. Yazdi, N. Neff, S.J. Elledge, J. Qin, BASC, a super complex of BRCA1-associated proteins involved in the recognition and repair of aberrant DNA structures, Genes Dev. 14 (2000) 927–939.
[15] M. Ababou, S. Dutertre, Y. Lecluse, R. Onclercq, B. Chatton, M. Amor-Gueret, ATM-dependent phosphorylation and accumulation of endogenous BLM protein in response to ionizing radiation, Oncogene 19 (2000) 5955–5963.
[16] M. Seigneur, V. Bidnenko, S.D. Ehrlich, B. Michel, RuvAB acts at arrested replication forks, Cell 95 (1998) 419–430.
[17] N.A. Ellis, J. Groden, T.Z. Ye, J. Straughen, D.J. Lennon, S. Ciocci, M. Proytcheva, J. German, The Bloom's syndrome gene product is homologous to RecQ helicases, Cell 83 (1995) 655–666.
[18] J.K. Karow, R.K. Chakraverty, I.D. Hickson, The Bloom's syndrome gene product is a 3′–5′ DNA helicase, J. Biol. Chem. 272 (1997) 30611–30614.
[19] J.K. Karow, A. Constantinou, J.L. Li, S.C. West, I.D. Hickson, The Bloom's syndrome gene product promotes branch migration of Holliday junctions, Proc. Natl. Acad. Sci. U. S. A. 97 (2000) 6504–6508.
[20] W. Wang, M. Seki, Y. Narita, E. Sonoda, S. Takeda, K. Yamada, T. Masuko, T. Katada, T. Enomoto, Possible association of BLM in decreasing DNA double strand breaks during DNA replication, EMBO J. 19 (2000) 3428–3435.
[21] N. Takao, H. Kato, R. Mori, C. Morrison, E. Sonada, X. Sun, H. Shimizu, K. Yoshioka, S. Takeda, K. Yamamoto, Disruption of ATM in p53-null cells causes multiple functional abnormalities in cellular response to ionizing radiation, Oncogene 18 (1999) 7002–7009.
[22] E. Sonoda, M.S. Sasaki, C. Morrison, Y. Yamaguchi-Iwai, M. Takata, S. Takeda, Sister chromatid exchanges are mediated by homologous recombination in vertebrate cells, Mol. Cell. Biol. 19 (1999) 5166–5169.
[23] K. Suzuki, S. Kodama, M. Watanabe, Recruitment of ATM protein to double strand DNA irradiated with ionizing radiation, J. Biol. Chem. 274 (1999) 25571–25575.
[24] K.K. Khanna, S.P. Jackson, DNA double-strand breaks: signaling, repair and the cancer connection, Nat. Genet. 27 (2001) 247–254.
[25] O. Bischof, S.H. Kim, J. Irving, S. Beresten, N.A. Ellis, J. Campisi, Regulation and localization of the Bloom syndrome protein in response to DNA damage, J. Cell Biol. 153 (2001) 367–380.
[26] L. Wu, S.L. Davies, N.C. Levitt, I.D. Hickson, Potential role for the BLM helicase in recombinational repair via a conserved interaction with RAD51, J. Biol. Chem. 276 (2001) 19375–19381.
[27] I. Szumiel, Monitoring and signaling of radiation-induced damage in mammalian cells, Radiat. Res. 150 (1998) S92–S101.
[28] M. Kupiec, Damage-induced recombination in the yeast *Saccharomyces cerevisiae*, Mutat. Res. 451 (2000) 91–105.
[29] H. Zou, R. Rothstein, Holliday junctions accumulate in replication mutants via a RecA homolog-independent mechanism, Cell 90 (1997) 87–96.
[30] S. Sengupta, S.P. Linke, R. Pedeux, Q. Yang, J. Farnsworth, S.H. Garfield, K. Valerie, J.W. Shay, N.A. Ellis, B. Wasylyk, C.C. Harris,

BLM helicase-dependent transport of p53 to sites of stalled DNA replication forks modulates homologous recombination, EMBO J. 22 (2003) 1210–1222.
[31] C. Morrison, E. Sonoda, N. Takao, A. Shinohara, K. Yamamoto, S. Takeda, The controlling role of ATM in homologous recombinational repair of DNA damage, EMBO J. 19 (2000) 463–471.
[32] D. Cortez, Y. Wang, J. Qin, S.J. Elledge, Requirement of ATM-dependent phosphorylation of brca1 in the DNA damage response to double-strand breaks, Science 286 (1999) 1162–1166.
[33] D.S. Lim, S.T. Kim, B. Xu, R.S. Maser, J. Lin, J.H. Petrini, M.B. Kastan, ATM phosphorylates p95/nbs1 in an S-phase checkpoint pathway, Nature 404 (2000) 613–617.
[34] S. Zhao, Y.C. Weng, S.S. Yuan, Y.T. Lin, H.C. Hsu, S.C. Lin, E. Gerbino, M.H. Song, M.Z. Zdzienicka, R.A. Gatti, J.W. Shay, Y. Ziv, Y. Shiloh, E.Y. Lee, Functional link between ataxia-telangiectasia and Nijmegen breakage syndrome gene products, Nature 405 (2000) 473–477.
[35] G. Chen, S.S. Yuan, W. Liu, Y. Xu, K. Trujillo, B. Song, F. Cong, S.P. Goff, Y. Wu, R. Arlinghaus, D. Baltimore, P.J. Gasser, M.S. Park, P. Sung, E.Y. Lee, Radiation-induced assembly of Rad51 and Rad52 recombination complex requires ATM and c-Abl, J. Biol. Chem. 274 (1999) 12748–12752.
[36] M.E. Moynahan, J.W. Chiu, B.H. Koller, M. Jasin, Brca1 controls homology-directed DNA repair, Mol. Cell 4 (1999) 511–518.

Available online at www.sciencedirect.com
SCIENCE DIRECT®
Mutation Research 557 (2004) 1–6
Genetic Toxicology and Environmental Mutagenesis
www.elsevier.com/locate/gentox
Community address: www.elsevier.com/locate/mutres

Genotoxicity of microcystin-LR in human lymphoblastoid TK6 cells

Li Zhan[a,b], Hiroko Sakamoto[a], Mayumi Sakuraba[a], De-Sheng Wu[b], Li-Shi Zhang[b], Takayoshi Suzuki[a], Makoto Hayashi[a], Masamitsu Honma[a,*]

[a] *Division of Genetics and Mutagenesis, National Institute of Health Sciences, 1-18-1 Kamiyoga, Setagaya-ku, Tokyo 158-8501, Japan*
[b] *West China School of Public Health, Sichuan University, Chengdu 610041, China*

Received 6 June 2003; received in revised form 22 September 2003; accepted 22 September 2003

Abstract

Toxic cyanobacteria (blue-green algae) water blooms have become a serious problem in several industrialized areas of the world. Microcystin-LR (MCLR) is a cyclic heptapeptidic toxin produced by the cyanobacteria. In the present study, we used human lymphoblastoid cell line TK6 to investigate the in vitro genotoxicity of MCLR. In a standard 4 h treatment, MCLR did not induce a significant cytotoxic response at <80 μg/ml. In a prolonged 24 h treatment, in contrast, it induced cytotoxic as well as mutagenic responses concentration-dependently starting at 20 μg/ml. At the maximum concentration (80 μg/ml), the micronucleus frequency and the mutation frequency at the heterozygous thymidine kinase (*TK*) locus were approximately five-times the control values. Molecular analysis of the *TK* mutants revealed that MCLR specifically induced loss of heterozygosity at the *TK* locus, but not point mutations or other small structural changes. These results indicate that MCLR had a clastogenic effect. We discuss the mechanisms of MCLR genotoxicity and the possibility of its being a hepatocarcinogen.

Keywords: Cyanobacteria; Microcystin-LR; Micronucleus test; TK-gene mutation

1. Introduction

Water pollution by cyanobacteria (blue-green algae) causes serious environmental and public health problems in several areas of the world [1–3]. Some genera, such as *Microsystis*, *Oscillatoria*, and *Anabaena* produce microcystines, cyclic heptapeptides, with potent hepatotoxic activity. Fifty different cyanobacterial microcystines have been discovered. They have caused the death of fish, birds, wild animals, and livestock [1,4] and sometimes have had adverse health effects on humans through contaminated residential water supplies [5,6].

Microcystin-LR (MCLR) is the most toxic microcystine. Only 1–2 μg MCLR given intraperitoneally is lethal to mice, with most accumulating in the liver [7,8]. While MCLR hepatotoxicity has been well documented in vitro and in vivo [9–12], few reports describe its genotoxicity. MCLR is not genotoxic in the Ames test, although cyanobacterial extracts are, both with and without metabolic activation [13]. In a human cancer cell line, on the other hand, MCLR induces point mutations, and it produces DNA fragmentation and degradation in mouse liver in vivo [14,15].

* Corresponding author. Tel.: +81-3-3700-1141x434; fax: +81-3-3700-2348.
E-mail address: honma@nihs.go.jp (M. Honma).

1383-5718/$ – see front matter © 2003 Elsevier B.V. All rights reserved.
doi:10.1016/j.mrgentox.2003.09.006

To evaluate the in vitro genotoxicity of MCLR, we used the in vitro micronucleus (MN) assay and the thymidine kinase (*TK*) gene mutation assay on treated human lymphoblatoid TK6 cells [16,17]. The *TK* gene mutation assay is capable of detecting a wide range of genetic damage, including gene mutations, large scale chromosomal changes, recombination, and aneuploidy. Most of the changes occur in human tumors and are presumably relevant to carcinogenesis. Use of a human cell line makes this genotoxicity evaluation appropriate for human hazard evaluation. Molecular analysis of the *TK*-mutants may help us understand the genotoxic mechanism of MCLR [18,19].

2. Materials and methods

2.1. Cells culture and chemical treatment

The TK6 human lymphoblastoid cell line has been described previously [18]. Cells were grown in RPMI1640 medium (Gibco-BRL, Life technology Inc., Grand Island, NY) supplemented with 10% heat-inactivated horse serum (JRH Biosciences, Lenexa, KS), 200 μg/ml sodium pyruvate, 100 unit/ml penicillin, and 100 μg/ml streptomycin. The cultures were incubated at 37 °C in a 5% CO_2 atmosphere with 100% humidity and maintained at densities ranging from 10^5 to 10^6 cells/ml.

MCLR (Cas.# 101043-37-2) was purchased from Wako Pure Chemical Co. (Tokyo, Japan) and dissolved in phosphate-buffered saline just before use. Prior to their exposure, the cells were cultured in CHAT (10 μM deoxycytidine, 200 μM hypoxanthine, 0.1 μM aminopterin, 17.5 μM thymidine) medium for 2 days to reduce the background mutant fraction. Cultures of 20 ml at 5.0×10^5 cells/ml and of 50 ml at 2.0×10^5 cells/ml were treated at 37 °C with serial dilution of MCLR for 4 h and 24 h, respectively. They were then washed once, re-suspended in fresh medium, and cultured in new flasks for the MN assay and *TK* gene mutation assay, or diluted to be plated for survival estimates.

2.2. MN assay

Forty-eight hours after exposure, the MN assay samples were prepared as previously reported [20]. Briefly, approximately 10^6 cells suspended in hypotonic KCl solution were incubated for 10 min at room temperature, fixed twice with ice-cold fixative (glacial acetic acid: methanol, 1:3), and then re-suspended in methanol containing 1% acetic acid. A drop of the suspension was placed on a clean glass slide and air-dried. The cells were stained with 40 μg/ml acridine orange solution and immediately observed with the aid of an Olympus model BX50 fluorescence microscope equipped with a U-MWBV band pass filter. At least 1000 intact interphase cells for each treatment were examined, and the cells containing MN were scored.

2.3. TK gene mutation assay

The TK6 cell cultures were maintained for 3 days after exposure to permit expression of the *TK* deficient phenotype. To isolate the *TK* deficient mutants, we seeded cells into 96-well microwell plates at 40,000 cells/well in the presence of 3.0 μg/ml trifluorothymidine (TFT). Cells from each culture were also plated at 1.6 cells/well in the absence of TFT for the determination of plating efficiency (PE). All plates were incubated for 14 days at 37 °C in a 5% CO_2, humidified incubator, and then scored for colony formation. Plates containing TFT were then re-fed with TFT, incubated for an additional 14 days, and scored for the appearance of slow-growing *TK* mutants. Mutation frequencies were calculated according to the Poisson distribution [21].

2.4. LOH analysis of TK mutants

Genomic DNA was extracted from *TK* mutant cells and used as a template for PCR. The PCR-based LOH analysis at human *TK* gene was described previously [19]. Two sets of primers were used to amplify the parts of exons 4 and 7 of the *TK* gene containing frameshift mutations. Another primer set for amplifying parts of the β-globin was also prepared. Quantitative-multiple PCR was subjected to co-amplification of the three regions and qualify and quantify the PCR products. They were analyzed with an ABI310 genetic analyzer (PE Biosystems, Chiba, Japan), and classified them into non-LOH, hemizygous LOH, or homozygous LOH mutants.

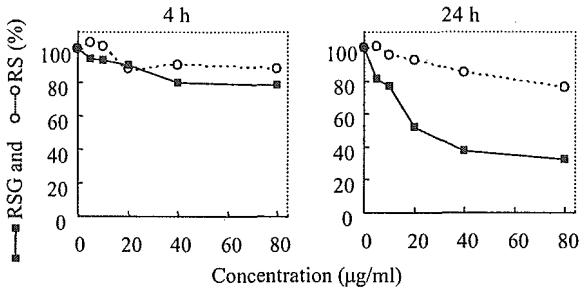

Fig. 1. Cytotoxic responses represented by RS and relative cell growth (RSG) of TK6 cells treated with MCLR for 4 or 24 h.

3. Results

3.1. Cytotoxic response to MCLR

TK6 cells were exposed to various doses of MCLR for 4 or 24 h. Fig. 1 shows cytotoxic responses; relative survival (RS) and relative suspension growth (RSG), which is relative cell growth during 72 h after exposure. Exposure to MCLR for 4 h did significantly affect RS or RSG. Exposure for 24 h, however, decreased RSG concentration-dependently, but did not significantly alter RS.

3.2. Genotoxic responses to MCLR

Exposure to MCLR for 24 h induced both MN and *TK* mutation in a concentration-dependent manner (Fig. 2). The maximum induction of MN and *TK* mutations were 4.8- and 5.1-times the control values. Two distinct phenotypic classes of *TK* mutants were generated. Normally growing (NG) mutants grew at the same rate as the wild type cells (doubling time 13–17 h), and slowly growing (SG) mutants grew at a slower rate (doubling time >21 h). NG mutants result mainly from intragenic mutations, while SG mutants result from gross genetic changes beyond the *TK* gene. The proportion of SG mutants increased in MCLR induced mutants, suggesting that MCLR was clastogenic.

3.3. Molecular analysis of TK mutants

Spontaneously arising and MCLR-induced *TK* mutants were isolated independently. The MCLR-induced

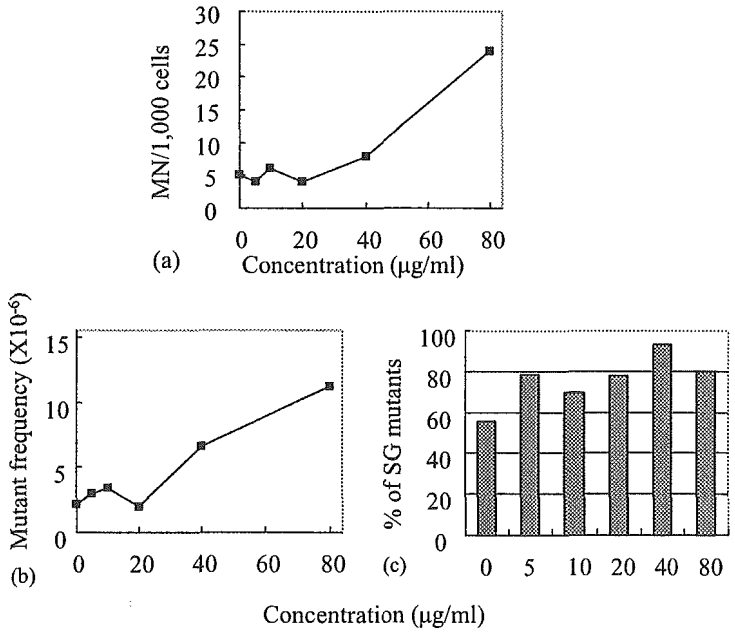

Fig. 2. MN induction (a), mutation frequency at *TK* locus (b), and percentage of slowly growing (SG) mutants (c) among TK-deficient mutants treated with MCLR for 24 h.

Table 1
Cytotoxic and mutational response to MCLR[a] and LOH analysis of TK-mutants

Treatment	Cytotoxic and mutational response			LOH analysis at *TK* gene			
	RSG (%)	MF ($\times 10^{-6}$)	% SG	No. analyzed	None LOH	Hemizygous LOH	Homozygous LOH
Spontaneous	100	2.19	56	56			
NG mutants				19	14 (74)	3 (16)	2 (11)
SG mutants				37	0 (0)	9 (24)	28 (76)
MCLR-induced	32.6	11.2	80	36			
NG mutants				9	4 (44)	5 (56)	0 (0)
SG mutants				27	0 (0)	10 (37)	17 (63)

[a] 80 μg/ml for 24 h.

mutants were produced by the treatment at 80 μg/ml for 24 h. The cytotoxicity (RSG), mutation frequency, and proportion of SG mutants by the treatment are shown in Table 1. We used PCR-based LOH analysis of genomic DNA from *TK* mutants to classify the mutants into 3 types; Non-LOH, hemizygous LOH, and homozygous LOH. We analyzed 58 spontaneous and 36 MCLR induced *TK* mutants, including NG and SG type (Table 1). Every SG mutant was a result of LOH regardless of the treatment, suggesting that SG mutants were always associated with gross genetic changes. Among the MCLR-induced mutants, 56% of NG mutants and 100% of SG mutants exhibited LOH. Every LOH in the NG mutants was hemizygous, and 63% of LOH in the SG mutants was homozygous. This is in contrast to spontaneous *TK* mutants, where the majority of spontaneous NG and SG mutants were non-LOH (74%) and homozygous LOH (76%), respectively. Fig. 3 shows the spectra of spontaneous and MCLR-induced *TK* mutants in TK6 cells, which were adjusted by considering % SG mutants. These data clearly indicate that MCLR induced LOH, but not point mutation or other small genetic changes.

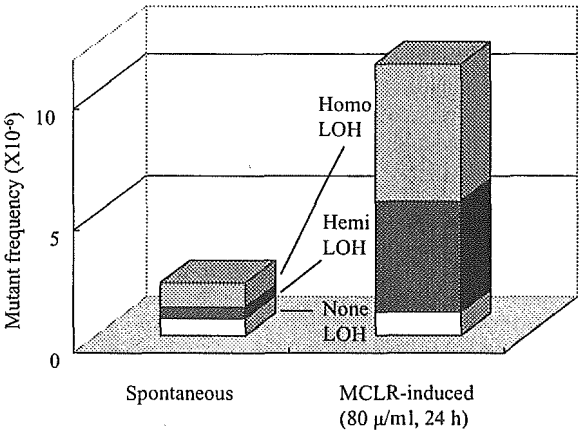

Fig. 3. Frequency and spectra of *TK* mutations in spontaneous and MCLR (80 μg/ml, 24 h) induced *TK* mutants in TK6 cells. The fraction of each mutational event was calculated by considering the ratio of NG and SG mutants and the result of molecular analysis (Table 1).

4. Discussion

Although MCLR causes severe hepatoxoxicity in mammals [9–12], its genotoxicity and carcinogenicity are inconclusive. Ding et al. [13] reported that microcystic cyanobacteria extract (MCE) significantly induced mutations in the Ames assay regardless of metabolic activation, although pure MCLR did not. Tsuji et al. [22,23] also failed to demonstrate MCLR genotoxicity in the Ames assay. On the other hand, MCLR has some genotoxic effects in mammalian cells. Ding et al [13] observed DNA damage in primary rat hepatocytes in comet assay, and Rao and Bhattacharya [14] found that MCLR could induce DNA fragmentation and strand breaks in mouse liver in vivo. Two studies reported the induction of chromosome aberrations and gene mutations in mammalian cells [15,24].

Our present study clearly demonstrated the in vitro genotoxicity of MCLR, which induced MN formation as well as gene mutations in human cells. A 24 h treatment was required, however, to express the effects. Although MCLR is toxic and highly lethal to